ISSN 1062-7391, Journal of Mining Science, 2018, Vol. 54, No. 4, pp. 541–549. © Pleiades Publishing, Ltd., 2018.
Original Russian Text © L.A. Nazarova, L.A. Nazarov, 2018, published in Fiziko-Tekhnicheskie Problemy Razrabotki Poleznykh Iskopaemykh, 2018, No. 4, pp. 11–20.

GEOMECHANICS

Geomechanical and Hydrodynamic Fields in Producing Formation in the Vicinity of Well with Regard to Rock Mass Permeability–Effective Stress Relationship

L. A. Nazarova and and L. A. Nazarov*

Chinakal Institute of Mining, Siberian Branch, Russian Academy of Sciences, Novosibirsk, 630091 Russia
**e-mail: naz@misd.ru*

Received June 11, 2018
Revised June 27, 2018
Accepted July 2, 2018

Abstract—The nonlinear model is developed to describe geomechanical and hydrodynamic fields in the vicinity of a vertical well in a fluid-saturated formation for the case when the permeability k depends on the effective stress σ_f by the exponential law. The analytical solutions are obtained for the porous–elastic and porous–elastoplastic modes of deformation of the well vicinity, based on which the change in the pressure and rate of flow under the variation of parameters characterizing the dependence $k(\sigma_f)$ is analyzed. It is found that the rate of flow exponentially decreases with an increasing horizontal stress of the external field; the permeability of the irreversible strain zone around the well decreases with the distance from the well boundary. The test scheme is proposed for permeability of samples with the center hole under side loading, and the experimental data interpretation procedure is put forward, which enables finding the empirical dependence $k(\sigma_f)$.

Keywords: Rock mass, porous–elastic and porous–elastoplastic deformation, effective stress, permeability, well, experiment, sample with center hole.

DOI: 10.1134/S1062739118043989

INTRODUCTION

The knowledge of reservoir rock properties in oil and gas fields is indispensable in solving many problems associated with petroleum exploration and development which include, but are not limited to the substantiation of efficient drilling and production strategies; production potential assessment of wells; production planning; interpretation of well-log data [1, 2]. The permeability (k) and porosity estimated by logging is assumed to be piecewise constant within the target pay interval [3–6]. Meanwhile, the laboratory testing of reservoir rocks [7, 8] and coal [9], as well as the field studies [10, 11] show that permeability varies with effective stress $\sigma_f = p + \sigma$ (p is the fluid pressure and σ is the mean normal stress in the rock matrix). As long as deformation is elastic, the $k(\sigma_f)$ dependence is well approximated [9, 12] by the exponential function:

$$k(\sigma_f) = k_0 \exp(\beta \sigma_f), \tag{1}$$

where k_0 is the permeability found in a standard way in core samples [13], and β is an empirical constant. At the post-limiting stage (plasticity and failure), permeability can either decrease [7] or increase [11] as the effective stress increases.

Drilling produces a heterogeneous stress field around the well [14] and zones of irreversible strain (failure) at depths [15], which leads to changes in the reservoir properties of rocks in the well vicinity. These effects are commonly taken into account by introducing a skin factor into the model (parameters of a local zone inferred from the pressure recovery curve [16–18]), but this conventional approximate approach is not always workable [19]. Various models of failure for reservoir engineering practices were discussed in [20, 21].

In this study, forward analytical solutions are obtained for a steady-state fluid flow toward a well in a rock mass in the conditions of stress-dependent permeability and porous–elastic or porous–elastoplastic deformation [22]. The solutions are used to constrain the empirical constant β in (1) from laboratory testing. Previously, an asymptotic solution was obtained [23] for a similar nonsteady problem in a porous–elastic formulation.

1. BOUNDARY PROBLEM FORMULATION

The modeling is performed for a vertical well of the radius r_0 penetrating a homogeneous fluid-saturated bed of the thickness h located at the depth H ($h << H$).

Geomechanical model. Let the horizontal stress of the natural field be equal, then the model is symmetrical and the stress state of rocks around the well in the cylindrical coordinates (r is the radius and θ is the polar angle) is described by a system of equations including [22]:
the equilibrium equation

$$\sigma_{rr,r} + \frac{\sigma_{rr} - \sigma_{\theta\theta}}{r} = 0\,; \tag{2}$$

the Cauchy equations

$$\varepsilon_{rr} = u_{,r}\,,\ \ \varepsilon_{\theta\theta} = \frac{u}{r}\,; \tag{3}$$

Hooke's law for porous–elastic deformation

$$\begin{aligned} \sigma_{rr} &= (\lambda + 2\mu)\varepsilon_{rr} + \lambda\varepsilon_{\theta\theta} - p\,, \\ \sigma_{\theta\theta} &= \lambda\varepsilon_{rr} + (\lambda + 2\mu)\varepsilon_{\theta\theta} - p\,, \end{aligned} \tag{4}$$

and the Mohr-Coulomb criterion for failure zones [24]

$$|\,\sigma_{rr} - \sigma_{\theta\theta}\,| = |\,\sigma_{rr} + \sigma_{\theta\theta}\,|\,\mathrm{tg}\varphi + 2\tau_c\,, \tag{5}$$

where σ_{rr}, $\sigma_{\theta\theta}$ and ε_{rr}, $\varepsilon_{\theta\theta}$ are the stress and strain tensor components; p is the pore fluid pressure; u is the radial displacement; λ and μ are the Lamé constants; φ is the internal friction angle; τ_c is the cohesion.

Fluid dynamic model. The steady-state fluid flow in the well vicinity is described with [25, 26]:
the continuity equation

$$(rv)_{,r} = 0 \tag{6}$$

and the linear Darcy law

$$v = -kp_{,r}/\eta\,, \tag{7}$$

where v and η are, respectively, the radial Darcy velocity and viscosity of the fluid; the permeability k is a function of effective stress according to (1).

Boundary conditions. Problem (1)–(7) is solved within the ring $D = \{r_0 \le r \le r_1\}$, with the following conditions at its internal and external boundaries:

$$\sigma_{rr}(r_0) = -p_0\,,\ \sigma_{rr}(r_1) = -S\,, \tag{8}$$

$$p(r_0) = p_0\,,\ p(r_1) = p_1\,, \tag{9}$$

where $S = q\sigma_V$ (q is the lateral pressure; $\sigma_V = \rho gH$ is the overburden pressure; ρ is the rock density; g is the acceleration due to gravity), the compressive stresses are assumed to be negative; during production $p_0 = p_a$ (p_a is the atmospheric pressure); during drilling $p_0 = \rho_0 gH$ (ρ_0 is the drilling mud density); p_1 is the pressure at the external boundary, $r = r_1$.

2. GEOMECHANICAL AND GEODYNAMIC FIELDS IN THE WELL VICINITY

Porous–elastic model. The common solution to system (2)–(4), reduced to an ordinary second-order equation, is:

$$\sigma_{rr}(r) = A - Br^{-2} - 2\delta\Phi(r),$$
$$\sigma_{\theta\theta}(r) = A + Br^{-2} + 2\delta[\Phi(r) - p(r)], \tag{10}$$

where $\delta = 1-2\nu$ (ν is Poisson's ratio); $\Phi(r) = r^{-2}\int_{r_0}^{r} p(\xi)\xi d\xi$. The constants A and B are found from boundary conditions (8):

$$A = c - p_0,\ B = r_0^2 c,\ c = \frac{2\delta\Phi(r_1) - S + p_0}{1 - r_0^2 / r_1^2},$$

at $r_0 << r_1$, we have $A = 2\delta\Phi(r_1) - S$. As follows from (10), the effective stress:

$$\sigma_f = 0.5(\sigma_{rr} + \sigma_{\theta\theta}) + p = A + (1-\delta)p. \tag{11}$$

The system of equations (1), (6) and (7) that describe pressure distribution in the study domain is reduced to the equation:

$$\frac{\partial}{\partial r}\left(r e^{\beta\sigma_f} \frac{\partial p}{\partial r} \right) = 0. \tag{12}$$

This equation allows separation of variables, with regard to (11), and has the general solution:

$$e^{\alpha_e p} = A_e + B_e \ln r,$$

where $\alpha_e = 2\nu\beta$.

With the constants A_e and B_e found from boundary conditions (9), we obtain:

$$p(r) = \frac{1}{\alpha_e}\ln\left[e^{\alpha_e p_0} + (e^{\alpha_e p_1} - e^{\alpha_e p_0})\frac{\ln(r/r_0)}{\ln(r_1/r_0)} \right], \tag{13}$$

then the well discharge (flow rate) is:

$$Q(\alpha_e) = F_e(\alpha_e) Q_0, \tag{14}$$

where $F_e(\alpha_e) = \exp(0.5\alpha_e A/\nu)(e^{\alpha_e p_1} - e^{\alpha_e p_0})/[\alpha_e(p_1 - p_0)]$; $Q_0 = 2\pi H k_0 (p_1 - p_0)/[\eta \ln(r_1/r_0)]$ is the flow rate at $\alpha_e = 0$ (Dupuit equation [26]). As expected, $Q(\alpha_e) = 0$ at $p_0 = p_1$, $F_e(0) = 1$.

Thus, the solution within porous–elastic model (1)–(4) at the steady flow to the well shows that the flow rate decreases exponentially at increasing horizontal stress S in the external field.

Porous–elastoplastic model. Modern production wells reach depths of 3–4 km [27] where the hoop stress $\sigma_{\theta\theta}$ is as high as 80–100 MPa [15], even if drilling uses heavy mud (ρ_0=1500–700 kg/m^3), which exceeds the ultimate strength for most of reservoirs [28]. Therefore, drilling induces zones of irreversible strain (failure) with altered reservoir properties around the well [7].

Let the criterion of equation (5) hold true for some combination of the values φ, τ_c, p_0, p_1 and S. The failure zone $D_p = \{r_0 \le r \le r_*\}$ forms in D, and the deformation is elastic within the subdomain $D_e = D / D_p$. Within D_p, the solution to (2), (5) and $(8)_1$ is found in terms of elementary functions:

$$\sigma_{rr}(r) = R_1(r) - p_0,$$
$$\sigma_{\theta\theta}(r) = R_1(r) - 2R_2(r) - p_0, \tag{15}$$

where $R_1(r) = \tau_c[1 - (r/r_0)^{\Omega}]/m$, $R_2(r) = [\tau_c (r/r_0)^{\Omega}]/(1-m)$, $m = \tan\phi$, $\Omega = 2m/(1-m)$.

In the elastic subdomain, the stresses σ_{rr} and $\sigma_{\theta\theta}$ are also expressed by equations (10), but the constants A and B are found from the continuity condition of stresses (10) and (15) at the boundary $r = r_*$, then, in D_e:

$$\sigma_{rr}(r) = \sigma_e - \frac{Br_*^2}{r^2} - 2\delta\Phi(r),$$
$$\sigma_{\theta\theta}(r) = \sigma_e + \frac{Br_*^2}{r^2} + 2\delta[\Phi(r) - p(r)], \tag{16}$$

where $\sigma_e = \delta p(r_*) - R_2(r_*) + R_1(r_*) - p_0$, $B = \delta p(r_*) - R_2(r_*) - 2\delta\Phi(r_*)$.

Failure zone size. Drilling velocity can reach 1 m/min [29]; therefore, it can be assumed that drilling in a thin fluid-saturated reservoir instantly induces a perturbed stress field—irreversible strain zone D_p in the well vicinity, provided that the strength criterion is fulfilled. For finding the radius r_* let $\delta = 0$ in $(16)_1$ and the condition $(8)_2$:

$$\left(\frac{r_*}{r_0}\right)^{\Omega} - m\left(\frac{r_*}{r_1}\right)^2 = (1-m)\left(m\frac{S-p_0}{\tau_c} + 1\right). \tag{17}$$

As the condition $r_* > r_0$ is satisfied within D_p, the right-hand side of transcendent equation (17) should 1 at $r_* << r_1$. Thus, the respective horizontal stress in the external field can be estimated as:

$$S > p_0 + \frac{\tau_c}{1-m}, \tag{18}$$

and the depth of drilling-induced failure is:

$$H > \frac{\tau_c}{g(1-m)(q\rho - \rho_0)}.$$

Figure 1 shows the dependence of r_* on the dimensionless value $s = (S - p_0)/\tau_c$ at different internal friction angles φ.

At the next step, the pressure distribution in the domain D is found assuming that the constant β in (1) takes different values in the zones of elastic and inelastic deformation:

$$\beta = \begin{cases} \alpha & r \in D_e, \\ \alpha_p & r \in D_p. \end{cases}$$

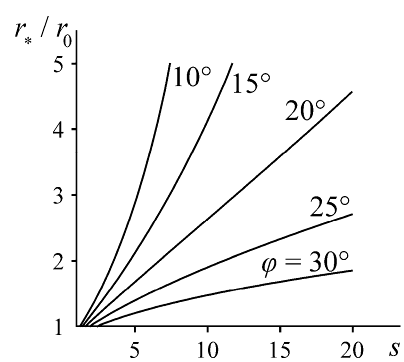

Fig. 1. Function $r_*(s)$ at different angles φ.

According to (16), the average stress σ in the subdomain D_e is pressure-dependent. It follows from (15) that σ in D_p varies as the known function of the radius. Therefore, equation (12) allows separation of variables everywhere in the domain D and has the analytical solution:

$$p(r)=\begin{cases}\ln[A_p+B_pG_p(r)], & r\in D_p,\\ \ln[A_e+B_eG_e(r)], & r\in D_e,\end{cases}$$

$G_e(r)=\exp\dfrac{-0.5\alpha_e\sigma_e}{\nu}\ln\dfrac{r}{r_*}$, $\quad G_p(r)=\displaystyle\int_{r_0}^{r}\exp[-\alpha_p\sigma_p(\xi)]\xi^{-1}d\xi$, $\quad \sigma_p(r)=R_1(r)-R_2(r)-p_0$. The unknown constants A_e, B_e, A_p and B_p are found from (9) and from the continuity conditions for pressure and filtration velocity at the interface of D_e and D_p:

$$p(r_*-0)=p(r_*+0)=p_*,\ v(r_*-0)=v(r_*+0).$$

Omitting cumbersome intermediate derivations, the final result is obtained as:

$$p(r)=\frac{1}{\alpha_p}\ln\left[e^{\alpha_p p_0}+(e^{\alpha_p p_*}-e^{\alpha_p p_0})\frac{G_p(r)}{G_p(r_*)}\right]\text{ at } r\in D_p; \tag{19}$$

$$p(r)=\frac{1}{\alpha_e}\ln\left[e^{\alpha_e p_*}+(e^{\alpha_e p_1}-e^{\alpha_e p_*})\frac{G_e(r)}{G_e(r_1)}\right]\text{ at } r\in D_e. \tag{20}$$

The pressure p_* at the boundary $r=r_*$ is found from the transcendent equation:

$$\alpha_pG_p(r_*)e^{\alpha_e p_*}+\alpha_eG_e(r_1)e^{\alpha_p p_*}=\alpha_eG_e(r_1)e^{\alpha_p p_0}+\alpha_pG_p(r_*)e^{\alpha_e p_1}. \tag{21}$$

Parametric analysis. The calculations were performed at $r_0=0.1$ m, $r_1=200$ m, $\nu=0.22$, $\tau_c=5$ MPa, $\varphi=12°$, $S=30$ MPa, and $p_0=0.1$ MPa; the values of p_1, α_e and α_p were varied. The permeability k is plotted in Fig. 2 for different α_p at $p_1=30$ MPa in the well vicinity. The increase in α_p leads to a reduction in k from the maximum at the well wall to the minimum at the failure zone boundary.

Figure 3 shows the pressure behavior at $p_1=20$ MPa and at different α_e and α_p. It is seen that the permeability decreases with increasing α_e, and the pressure in the well vicinity grows correspondingly (Fig. 3a). Note that the permeability is continuous at the boundary $r=r_*$ at $\alpha_p=\alpha_e$, and the pressure is a smooth function therefore.

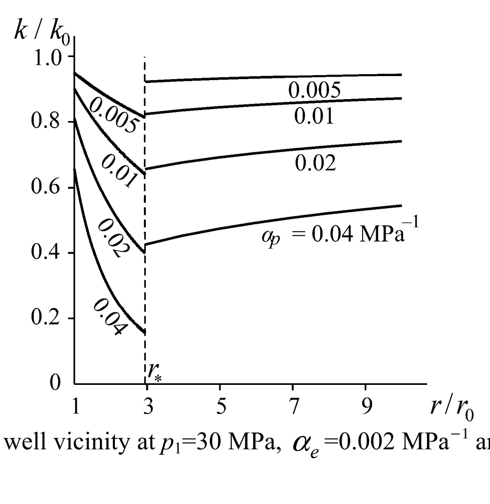

Fig. 2. Permeability in the well vicinity at p_1=30 MPa, α_e=0.002 MPa^{-1} and different values of α_p.

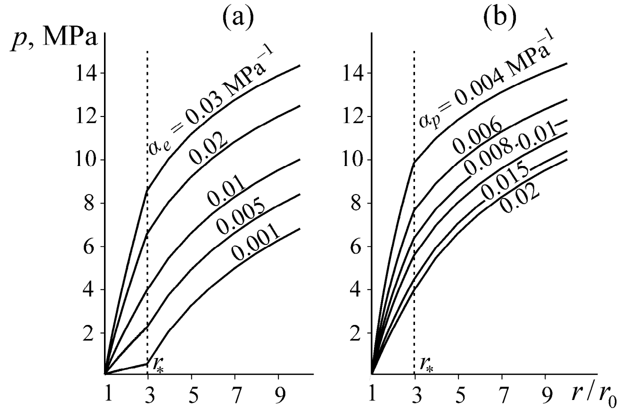

Fig. 3. Pressure in the well vicinity at (a) $\alpha_p = 0.01\ \text{MPa}^{-1}$ and (b) $\alpha_e = 0.02\ \text{MPa}^{-1}$.

The well flow rate is found using (19):

$$Q(\alpha_p) = Q_p F_p(\alpha_p),$$

$$Q_p = 2\pi H \frac{k_0}{\eta} \frac{p_* - p_0}{\ln \dfrac{r_*}{r_0}}, \quad F_p(\alpha_p) = \frac{e^{\alpha_p p_*} - e^{\alpha_p p_0}}{\alpha_p (p_* - p_0)} \frac{\ln \dfrac{r_*}{r_0}}{G_p(r_*)}.$$

The dependence of the relative flow rate F_p on the pressure at the well wall is plotted in Fig. 4 for $\alpha_e = 0.02\ \text{MPa}^{-1}$, $S = 30$ MPa and different α_p. Note that Q is expectedly decreases with increasing α_p and grows nonlinearly with elevating p_1.

3. METHOD OF DETERMINING EMPIRICAL DEPENDENCE OF PERMEABILITY ON EFFECTIVE STRESS BY EXPERIMENTAL DATA

Reservoir properties are determined from core testing as a rule [13]. The experimental scheme for determining empirical relationship of permeability and effective stress is analogous: the steady-state flow along the axis of a sample exposed to triaxial or less often biaxial compression [7, 9].

The radial permeability can be obtained in two main ways [1, 2, 30]: standard procedure applied to samples drilled out of a core orthogonally to its axis; radial flow of injected fluid through a hole made at the sample center.

Each way has its advantages and shortcomings, but in the first method, the linear dimensions of a sample are diminished by an order of magnitude. This greatly complicates penetration testing under loading using standard equipment (especially, at the post-limiting stage).

In this study, we consider the second method of finding the empirical constant β in (1) under porous–elastic and porous–elastoplastic deformation. Leaving technical details of the testing procedure aside, the experimental program and the data processing work flow are outlined below.

3.1. Experimental Program

1. Several samples are made from a full-size core; some are used to determine Poisson's ratio ν and strength characteristics (internal friction angle φ and cohesion τ_c) following the conventional procedures [31–33]. The ultimate radial stress $S_L = \tau_c / (1 - \tan\varphi)$ is estimated from equation (18).

2. A constant fluid pressure p_0 is created in a hole of the radius r_0 drilled at the center of a cylindrical sample (radius r_1, height H).

3. Stepwise increasing radial compression S_i ($i = 0, ..., n$) is applied to the lateral sample surface ($S_n < S_L$). The rate W_i of the steady flow is recorded at each loading step i.

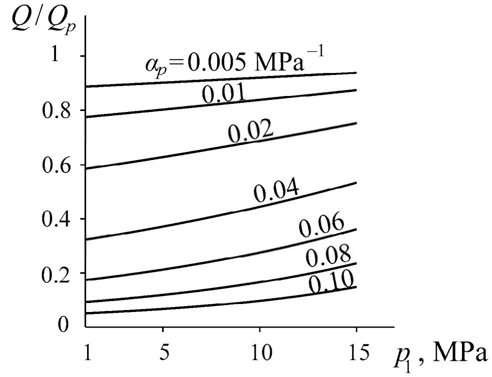

Fig. 4. Function $F_p(p_1)$ at $\alpha_e = 0.02$ MPa^{-1} and $S = 30$ MPa.

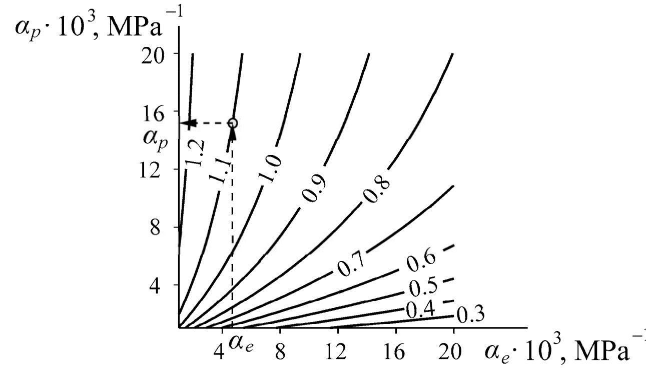

Fig. 5. Lines of the function T at $S_* = 30$ MPa, $p_0 = 15$ MPa, $p_1 = 0.1$ MPa, $r_0 = 2.5$ mm, and $r_1 = 25$ mm.

4. The radial stress is increased to $S_* > S_L$, and the flow rate W_* is measured on the lateral surface of the sample.

3.2. Data Interpretation

The stress and pressure fields in the tested samples are described by equations (1)–(8), which allows using the solutions (at $r_0 << r_1$) obtained within the limits of the porous–elastic and porous–elastoplastic models.

At $S < S_L$, the flow to the lateral surface of the sample is found according to (13):

$$Q_e(S) = 2\pi H \frac{k_0}{\eta} \frac{e^{\alpha_e p_0} - e^{\alpha_e p_1}}{\alpha_e \ln(r_1 / r_0)} \exp\left[\alpha_e \frac{2\delta\Phi(r_1) - S}{2\nu}\right],$$

wherefrom $Q_e(S) = Q_e(0)\exp(-\alpha_e S / 2\nu)$. Assuming $Q_e(0) = W_0$ in the latter relation, the value α_e can be estimated by the least square method:

$$\alpha_e = \frac{2\nu \sum_{i=1}^{n} S_i \ln(W_i / W_0)}{\sum_{i=1}^{n} S_i^2}.$$

At $S > S_L$, the flow rate Q_p at the surface $r = r_1$ is found from the pressure distribution in the subdomain D_e (20):

$$Q_p(S,\alpha_e,\alpha_p) = Q_e(0) T(\alpha_e,\alpha_p) \exp\frac{-\alpha_e S}{2\nu}, \quad T(S,\alpha_e,\alpha_p) = \frac{e^{\alpha_e p_*} - e^{\alpha_e p_1}}{e^{\alpha_e p_0} - e^{\alpha_e p_1}} \frac{\ln(r_1 / r_0)}{\ln(r_1 / r_*)},$$

where p_* and r_* implicitly depend on α_p and S (17), (21). Thus, with the known α_e, the empirical parameter α_p is found from the equation:

$$T(S_*,\alpha_e,\alpha_p) = \frac{W_*}{W_0} \exp\frac{\alpha_e S_*}{2\nu}. \tag{22}$$

Figure 5 demonstrates the one-valued solvability of (22): the straight line $\alpha_e = \text{const}$ has a single intersection with each line of the function T in the cross-section $S_* = \text{const}$.

Note that within the analyzed porous–elastic and porous–elastoplastic models, α_e and α_p are determined without regard to the fluid viscosity η and permeability k_0.

CONCLUSIONS

Drilling in producing formations initiates concentration zones of stresses potentially higher than ultimate strength. The latter conditions formation of irreversible strain zones with altered filtration properties. Within the framework of the porous–elastic and porous–elastoplastic models, the analytical solutions are obtained, which describe the distribution of steady-state geomechanical and geodynamic fields in the well vicinity under condition that permeability k depends on effective stress σ_f.

The dimensions of the failure zones as well as their depth of origin are estimated using the Mohr–Coulomb criterion. The numerical analysis has provided relationships between flow rate, permeability, and pressure under variation in the horizontal component S of the external stress and and parameters characterizing the dependence $k(\sigma_f)$ in the zones of elastic deformation and failure. Specifically, it is found that the flow rate increases at decreasing S and increasing external pressure. The filtration test setup is developed for cylindrical samples with a central hole, and, using the obtained solution, the experimental data processing procedure is proposed for determination of the parameters in the dependence $k(\sigma_f)$.

FUNDING

The study was carried out in the framework of the Basic Research Project, State Registration No. AAAA-A17-117122090002-5.

REFERENCES

1. Fjaer, E., Holt, R. M., Horsrud, P., et al., *Petroleum Related Rock Mechanics*, Elsevier, 2008.
2. Dake, L.P. *The Practice of Reservoir Engineering*, Elsevier, 2001.
3. Dakhnov, V.N., *Geofizicheskie metody opredeleniya kollektorskikh svoistv i neftegazonasyscheniya gornykh porod* (Geophysics for Estimation of Porosity, Permeability, and Fluid Saturation of Reservoir Rocks), Moscow: Nedra, 1985.
4. Lyons, W., Plisga, G., Lorenz, M., *Standard Handbook of Petroleum and Natural Gas Engineering*, Gulf Professional Publishing, 2015.
5. Nazarova, L.A., Nazarov, L.A., Epov, M.I., and El'tsov, I.N., Evolution of Geomechanical and Electro-Hydrodynamic Fields in Deep Well Drilling in Rocks, *J. Min. Sci.*, 2013, vol. 49, no. 5, pp. 704–714.
6. Yeltsov, I.N., Nazarova, L.A., Nazarov, L.A., Nesterova, G.V., Sobolev, A.Yu., and Epov, M.I., Geomechanics and Fluid Flow Effects on Electric Well Logs: Multiphysics Modeling, *Russian Geology and Geophysics*, 2014, vol. 55, no. 5–6, pp. 978–990.
7. Holt, R.M., Permeability Reduction Induced by a Nonhydrostatic Stress Field, *SPE Formation Evaluation*, 1990, no. 12, pp. 444–448.
8. Ghabezloo, S., Sulem, J., Guedon, S., and Martineau, F. Effective Stress Law for the Permeability of a Limestone, *Int. J. of Rock Mechanics and Mining Science*, 2009, vol. 46, pp. 297–306.
9. Espinoza, D.N., Vandamme, M., Pereira, J.-M., et al., Measurement and Modeling of Adsorptive–Poromechanical Properties of Bituminous Coal Cores Exposed to CO_2: Adsorption, Swelling Strains, Swelling Stresses and Impact on Fracture Permeability, *Int. J. of Coal Geology*, 2014, vol. 134–135, pp. 80–95.
10. Schutjens, P.M. T.M., Hanssen, T.H., Hettema, M.H.H., et al., Compaction-Induced Porosity/Permeability Reduction in Sandstone Reservoirs: Data and Model for Elasticity-Dominated Deformation, *SPE Reservoir Evaluation & Engineering*, 2004, vol. 7, no. 3, 202–216.
11. Zhu, W., Montesi, L., and Wong, T.-F. Characterizing the Permeability-Porosity Relationship during Compactive Cataclastic Flow, *42nd U.S. Rock Mechanics Symposium*, *USRMS*, San Francisco: ARMA, 2008.

12. Connell, L.D., Lu, M., and Pan, Z., An Analytical Coal Permeability Model for Tri-Axial Strain and Stress Conditions, *Int. J. of Coal Geology*, 2010, vol. 84, pp. 103–114.
13. *GOST 26450.2–85. Porody gornye. Metod opredeleniya koeffitsienta absolyutnoi gazopronitsaemosti pri statsionarnoi i nestatsionarnoi filtratsii* (State Standard. Working document 26450.2–85. Rocks. A Method for Determination of Absolute Gas Permeability at Steady and Nonsteady Flow), Moscow: Izd. Standartov, 1985.
14. Zoback, M.D., *Reservoir Geomechanics*, Cambridge University Press, 2010.
15. Yeltsov, I.N., Nazarov, L.A., Nazarova, L.A., Nesterova, G.V., and Epov, M.I., Logging Interpretation Taking into Account Hydrodynamical and Geomechanical Processes in an Invaded Zone, *Doklady Earth Sci.*, 2012, vol. 445, no. 2, pp. 1021–024.
16. Mishchenko, I.T., *Skvazhinnaya dobycha nefti* (Oil Production), Moscow: Neft Gaz, 2003.
17. Khisamov, R.S., Suleimanov, E.I., Farkhullin, R.G., et al., *Gidrodinamicheskie issledovaniya skvazhin i metody obrabotki rezul'tatov izmerenii* (Well Testing and Methods for Data Processing), Moscow: VNIIOENG, 2000.
18. Mufazalov, R.Sh., Skin Factor: Basic Relationships and Interplay Between Fluid Dynamic Parameters of a Zoned Reservoir and a Well, *ROGTEC*, 2015, pp. 76–90.
19. Medvedev, A.I. and Boganik, V.N., How to Determine the Skin Factor, *Geolog., Geofiz. Razrab. Neftya. Gaz. Mestorozhd.*, 2004, no. 5, pp. 42–45.
20. Penkovsky, V.I. and Korsakova, N.K., Modeling Hydraulic Fracture: Phenomenological Approach, *PMTF*, 2015, vol. 56, no. 5, pp. 139–148.
21. Nikolaevsky, V.N., *Geomekhanika. Sobranie trudov. Tom 1: Razrushenie i dilatansiya. Neft' i gaz. Seriya sovremennye neftegazovye tekhnologii* (Geomechanics. A collection of papers. Book 1: Failure and Dilatancy. Oil and gas. Series of Advanced Oil and Gas Technologies), Izhevsk: Izd. IKI, 2010.
22. Coussy, O., *Mechanics and Physics of Porous Solids*, John Wiley & Son Ltd, 2010.
23. Shelukhin, V.V. and Yeltsov, I.N., Wellbore Zone Dynamics Related to Drilling in a Porous Elastic Reservoir, *Geofiz. Zh.*, 2012, vol. 34, no. 4, pp. 265–272.
24. Jaeger, J.C., Cook, N.G.W., and Zimmerman, R., *Fundamentals of Rock Mechanics*, Wiley, 2007.
25. Harindra, J.F., *Handbook of Environmental Fluid Dynamics*, Vol. 1: Overview and Fundamentals, CRC Press, 2012.
26. Kochin, N.E., Kibel, I.A., and Roze, N.V., *Teoreticheskaya gidromekhanika. Chast' 1* (Theoretical Fluid Dynamics, Part 1), Moscow: Fizmatgiz, 1963.
27. Kalinin, A.G., *Burenie neftyanykh i gazovykh skvazhin* (Drilling of Oil and Gas Wells), Moscow: TsentrLitNefteGaz, 2008.
28. Dortman, N.B., *Fizicheskie svoistva gornykh porod i poleznykh iskopaemykh* (Physical Properties of Rocks and Mineral Resources), Moscow: Nedra, 1984.
29. http:.permneft-portal.ru/newspaper/articles/rekord-v-prokhodke (Last Access 10 June 2018)
30. Bradley, H.B., *Petroleum Engineering Handbook: Richardson, TX, Society of Petroleum Engineers*, 1987.
31. *GOST 21153.2-84. Porody gornye. Metody opredeleniya predela prochnosti pri odnoosnom szhatii* (State Standard. Working document GOST 21153.2-84. Rocks. Methods for Determination of Ultimate Strength at Unconfined Compressive Stress), Moscow: Izd. Standartov, 1984.
32. *GOST 21153.3-85. Porody gornye. Metody opredeleniya predela prochnosti pri odnoosnom rastyazhenii* (State Standard. Working document GOST 21153.3-85. Rocks. Methods for Determination of Ultimate Strength at Unconfined Tensile Stress), Moscow: Izd. Standartov, 1985.
33. *GOST 28985-91. Porody gornye. Metody opredeleniya deformatsionnykh kharakteristik pri odnoosnom szhatii* (State Standard. Working document GOST 28985-91. Rocks. Methods for Determination of Strain Parameters at Unconfined Compressive Stress), Moscow: Izd. Standartov, 1991.